IEEE Access
Multidisciplinary | Rapid Review | Open Access Journal

Received December 29, 2020, accepted January 11, 2021, date of publication January 20, 2021, date of current version February 12, 2021.

Digital Object Identifier 10.1109/ACCESS.2021.3053054

Graph Regularized Hierarchical Diffusion Process With Relevance Feedback for Medical Image Retrieval

LIMING XU[1,2], XIAOPENG YAO[1,3], LISHA ZHONG[1], JIANBO LEI[1,4], AND ZHIWEI HUANG[1,3]

[1]School of Medical Information and Engineering, Southwest Medical University, Luzhou 646000, China
[2]Chongqing Key Laboratory of Image Cognition, College of Computer Science and Technology, Chongqing University of Posts and Telecommunications, Chongqing 400065, China
[3]Central Nervous System Drug Key Laboratory of Sichuan Province, Luzhou 646000, China
[4]Center for Medical Informatics, Peking University, Beijing 100191, China

Corresponding author: Zhiwei Huang (hzwnet@swmu.edu.cn)

This work was supported by the National Natural Science Foundation of China (Grant No. 61971079), the Doctoral Research Innovation Project of Chongqing (Grant No. CYB19173), the Science and Technology Program of Sichuan (Grant No. 2020YJ0151, 2020YFQ0025) and the education Project of Sichuan (Grant No. 18ZA0514.)

ABSTRACT Befitting from the interpretability and the capacity in capturing the underlying manifold structure, diffusion process (DP) has attracted increasing attention in the field of image retrieval. Within it, hierarchical diffusion process (HDP) has achieved satisfactory results in retrieved performance and complexity. However, the existing hierarchical diffusion process methods only diffuse the affinity values in low-level visual space without considering the high-level semantic information, which cause the problem of semantic gap. To overcome these problems, we propose a Graph Regularized Hierarchical Diffusion Process (GRHDP) method with relevance feedback, and apply it to retrieve medical images. The proposed algorithm firstly establishes a hierarchical structure of the images in medical image database and spreads the affinity values among query images and top-layer images by graph regularization diffusion. Then relevance feedback is introduced to adjust the similarity between query images and retrieved images in top layer, and the affinity values are diffused again according to labeled information of feedback. Finally, the similarity between queries and others in database can be obtained by interpolating the diffused results on the top layer from top to bottom. The experimental results show that our proposed GRHDP with relevance feedback has achieved better retrieval performance than manifold ranking and regularized diffusion process (RDP) when returning top retrieved images.

INDEX TERMS Medical image retrieval, graph regularization, diffusion process, hierarchical structure, relevance feedback, semantic gap.

I. INTRODUCTION

Image retrieval technology has been rapidly developed for its important value in quickly retrieving needed images from large scale images. Within it, the text-based image retrieval [1] method which is a traditional retrieval method and mainly uses the manual keywords to determine the similarity among images has achieved satisfactory results. Although this traditional image retrieval is easy to understand and simple to implement, it still has two disadvantages: manual labels' subjectivity and high workload. To address these problems, researchers have proposed content-based image retrieval [2] method, which extracts low-level features (e.g., texture, color, contrast and sharpness) to retrieve images.

With the development of machine learning and manifold learning [3]–[5], content-based image retrieval has been a widely-used technology in large-scale image search task. In order to solve the curse of dimensionality, some [6], [7] proposed to reduce data dimensions by dimensionality reduction using manifold learning to further achieve effective retrieval. These methods obtain the retrieved results by ranking pairwise similarity computed in Euclidean conventionally. However, the intrinsic relationship cannot be preserved well using pairwise similarities. Then,

The associate editor coordinating the review of this manuscript and approving it for publication was Yin Zhang.

[8] proposed to use manifold ranking to enhance the relationship among images in context. On the basis of it, many improved methods [9]–[13] have been proposed and reached higher performance.

Similar with the manifold-based retrieval method, the diffusion process-based retrieval methods also focus on capturing the underlying manifold structure of images, and improve retrieved results. Most of them conduct the affinity graph where the connected edge can be computed by the Gaussian kernel function [14]–[17]. Apart from the standard graph, some have proposed to embed the variant graphs into diffusion process [18]–[22]. These diffusion process methods mainly model the underlying manifold structure of images to construct the affinity graph, and then diffuse the pairwise affinity values to other images along the reachable path of the graph.

Despite the progress made by diffusion process methods, there still remains two main challenges: (1) insufficient consideration about high-level semantic information and (2) semantic gap problem. To be specific, most diffusion process-based retrieve methods only diffuse the affinity values among images represented by low-level visual features without considering high-level semantic information. **Semantic gap** problem in this paper refers that understanding of computer is different from that of human beings. Simply put, it indicates that the retrieved image may be not desired for user.

Inspired by these two points, we, in this paper, propose Graph Regularized Hierarchical Diffusion Process (GRHDP) method with relevance feedback for medical image retrieval. Our proposed method firstly embeds all the images into a hierarchical structure by exploiting the algebraic multigrid [23] and manifold learning. Next, only a handful of images are used for diffusion process, and relevance feedback [24] is utilized to obtain high-level semantic information in the view of users. Finally, the diffused similarity measure is interpolated from top to bottom. The main contributions of this work can be summarized as follows:

- We propose Graph Regularized Hierarchical Diffusion Process (GRHDP) method for medical image retrieval. The proposed GRHDP decreases computational complexity in an interpretable way and achieves $O(N^2)$ time complexity with theoretical guarantee.
- We design a graph regularized hierarchical diffusion similarity to capture semantic relationship of medical images, which has been proved that it can preserve the underlying manifold structure of images.
- We incorporate relevance feedback to address the semantic gap and improve retrieval performance.
- The experimental results show that GRHDP have gained better retrieved performance than recent state-of-the-art manifold or diffusion process retrieval methods.

The remainder of this article is organized as follows. Section II introduces the procedure of diffusion process, and illustrates the effects on regularized diffusion process method. In section III, we describe the diffusion process of proposed algorithm and present optimization. Section IV provides the analysis of complexity. Extensive experimental results are presented in section V. Besides, we conclude our work and outline future work in section VI.

II. RELATED WORK

Comparing with text-based retrieval methods, the content-based method require less manual intervention and workload. Considering this, the content-based retrieval method has attracted increasing attention in image retrieval task. At present, the deep learning-based retrieval methods [25]–[28] have yield promising performance than traditional methods, but they are suffering poor interpretability and complexity analysis. Considering these, manifold preservation and diffusion process are introduced into large-scale images retrieval. These two methods are trying to capture and preserve underlying manifold structure in an interpretable way, and they can also achieve good retrieval performance and can be interpreted. In order to inherit the advantages of manifold preservation, diffusion process is considered to achieve efficient retrieval. Thus, we mainly focus on diffusion process-based retrieval methods in this paper.

Diffusion process-based retrieval method can be regarded as a variant of manifold-based method, and some related issues, variants and experimental results are summarized in [20]. It has been developed in recent years and there are several representative methods. Wang *et al.* [18] constructed an original graph and introduced a novel similarity metric into diffusion process based on the shortest path. It achieve satisfactory retrieval results and efficient retrieval time. Then, it has demonstrated that the retrieval performance of diffusion process using tensor product graph outperforms than that using original graph in recent studies of image retrieval [16], [17]. In order to further clear and quantify manifold structure of diffusion process, Yang *et al.* [19] used tensor product graph to capture the high-order information to further improve retrieval performance. Besides, Bai *et al.* [21] proposed a regularized diffusion process method which optimizes and improves tensor product graph [19] to reach better retrieval performance. At the same time, it explains that diffusion process on tensor product graph can preserve underlying relationship. Then, Bai *et al.* [22] proposed regularized ensemble diffusion and positive weight learning way to suppress negative impacts of noisy similarities.

Although some improved diffusion process-based image retrieval algorithms have been proposed, there are still two major challenges. Firstly, most diffusion process-based hashing methods only diffuse the affinity values among images represented by low-level visual features, but they ignore high-level semantic information. Then, understanding of computer is different from that of human beings, which may cause the semantic gap problem. That is to say, the the retrieved image may not be desired for user.

To address these problems, we made following three efforts. Firstly, we proposed a graph regularized hierarchical

diffusion process to capture the underlying manifold structure and reduce the time complexity. With in it, hierarchical framework and graph regularization are incorporated. The former ensures the convergence and complexity reduction with theoretical guarantee, and the latter ensures manifold structure preservation. To be specific, graph regularization is used to construct the relationship among images in dataset and smooth each pairwise relationship with tensor graph Laplacian. Secondly, the users' relevance feedback is taken into account to overcome the semantic gap problem (i.e., inconsistency between machine understanding and human cognition), which tries to ensure that the retrieved images are desired for users.

The most related work to ours is RDP model [21], which also uses regularization item to constrain the diffusion process. But it suffers from the high computation cost, and it spreads the similarity among images in the low-level visual feature space of images without considering the high-level semantic information. In our work, we establish a hierarchical structure to reduce time complexity and improve the computational efficiency, and use graph regularization for better manifold structure preservation. Besides, the relevance feedback is considered for a higher users' acceptance. These three improvements constitute the proposed GRHDP.

III. GRAPH REGULARIZED HIERARCHICAL DIFFUSION PROCESS WITH RELEVANCE FEEDBACK

Considering high computational cost of diffusion process-based image retrieval method which only utilizes the low-level visual feature to diffusing the affinity values among images, we propose GRHDP with the introduction of relevance feedback and high-level semantic information for medical image retrieval. It firstly selects some representative samples from database to construct a bottom-to-top hierarchical structure. Then the query image and top-layer images will be used to construct the graph, and the similarity is diffused along the path of graph by using RDP. Next, the users mark positive correlation or negative correlation according to the diffused results, and update iterative diffusion by adding the semantic information to obtain the similarity values of query image and top-layer images. Finally, these similarity values can be obtained through the hierarchical structure by interpolating between query image and all images in database. The detailed explanation of each operation is shown below.

A. HIERARCHICAL STRUCTURE

The existing image retrieval methods based on diffusion process have resulted in high computational cost with the increment of image scale. In order to reduce influence on retrieval speed when processing large-scale image retrieval, our method combine manifold learning and algebraic multi-grid to establish hierarchical structure for images in image library [29], which can reduce actual images for diffusion process. One of the key idea of our method is hierarchical structure which is based on the basis of

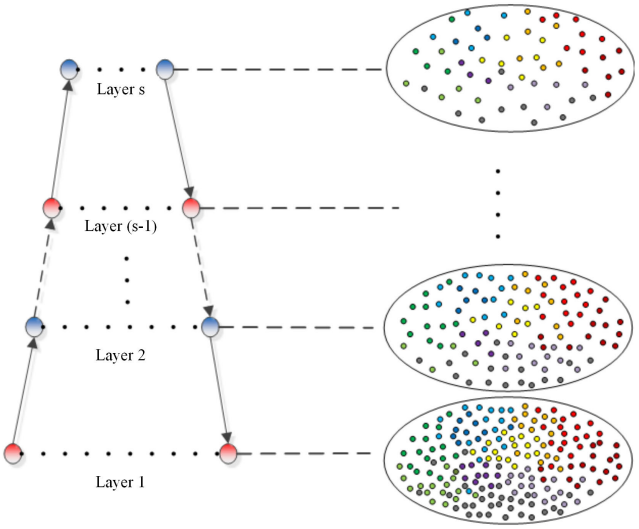

FIGURE 1. The hierarchical structure of images.

manifold hypothesis that assumes images in image library are distributed on a manifold structure. The locally adjacent images of manifold structure have similar characteristics, so representative images can be selected from similar images in local neighbor.

The selected representative images on the current layer will be delivered to upper layer to select next batch representative images. Analogously, the images of the next layer are processed in the same way as the last layer does. Finally, all the images will be formed into a bottom-to-top pyramidal hierarchical structure. Within it, the top-layer images denote the most representative images, which represent the main regional structure of image dataset. The bottom-layer image are all images in image dataset [30]–[32]. Figure 1 shows an overview of setting up the hierarchical structure of images.

Let $X = \{x_1, x_2, \ldots, x_n\} \in R^{m\times n}$ be image dataset, where n denotes image number and m represents feature dimensions of each image x_i. According to [29], [32], the designed hierarchical structure based on manifold learning and algebraic multi-grid is developed as follows:

(1) Construct k nearest neighbor graph $G^{[1]}(V^{[1]}, W^{[1]})$. $V^{[1]}$ denoted nodes indicates all images in the image library and $W^{[1]}$ denotes the edge affinity matrix. The affinity matrix $W^{[1]} = [W_{ij}^{[1]}]_{n\times n}$ is constructed by kernel function:

$$W_{ij}^{[1]} = \begin{cases} \exp\left(-\left\|x_i - x_j\right\|_2 / \sigma_1^2\right), & x_j \in N_k\left(x_i\right) \ or \ x_i \in N_k\left(x_j\right) \\ 0, & otherwise \end{cases} \tag{1}$$

where σ_1 denotes the parameter of the kernel function, $N_k(x_i)$ and $N_k(x_j)$ denote the k nearest neighbor set of images x_i and x_j, respectively;

(2) Select representative images. A bottom-to-top hierarchical structure of image is constructed by selecting representative images, where the selected images are strongly connected to unselected images on each layer. The strong or weak connection between two images is measured by using

the similarity metric in [30] and [31], which is essentially 0-1 matrix. The strong connection between pairwise images must satisfy:

$$W_{ij}^{[s]} \geq \theta * \ Max_{k \neq i} \left\{ W_{ik}^{[s]} \right\} \ , \ 0 < \theta \leq 1 \tag{2}$$

with $s = \{1, 2, \ldots, M\}$. M denotes the number of layer, and θ is the strength threshold. When Eq.(2) is satisfied, the image x_i is selected as representative images if the degree of its corresponding node is larger than the degree of corresponding node of image x_j. Otherwise the image x_j is selected as representative images;

(3) Calculate the affinity matrix $W^{[s]}$. After selecting the representative images on the s-th layer, a similarity transformation matrix is established to transform the affinity between two adjacent layers, which avoids re-calculating affinity matrix of images on the s-th layer [30], [32]. Similarity transformation matrix $Q^{[s-1]}$ which transforms affinity matrix $W^{[s-1]}$ from the $(s-1)$-th layer to the s-th layer to obtain affinity matrix $W^{[s]}$ can be defined:

$$\begin{cases} Q_{ik}^{[s-1]} = \dfrac{W_{ik}^{[s-1]}}{\sum_k W_{ik}^{[s-1]}}, & x_i \notin V^{[s]} \ , \ x_k \in V^{[s]} \\ \begin{cases} Q_{ii}^{[s-1]} = 1 \\ Q_{ij}^{[s-1]} = 0 \end{cases}, & x_i \in V^{[s]} \ , \ j \neq i \end{cases} \tag{3}$$

where $V^{[s]}$ denotes the image set of the s-th layer. When defining the transformation matrix Q and selecting the representative images V, the affinity matrix of representative images in the s-th layer can be calculated according to:

$$W^{[s]} = \left(Q^{[s-1]} \right)^T W^{[s-1]} Q^{[s-1]} \tag{4}$$

Therefore, the affinity matrix of representative images in each layer can be computed using:

$$W^{[s]} = \left(Q^{[s-1]} \right)^T \cdots \left(Q^{[1]} \right)^T \left(Q^{[0]} \right)^T W^{[0]} Q^{[0]} Q^{[1]} \ \cdots \ Q^{[s-1]} \tag{5}$$

B. GRAPH CONSTRUCTION AND DIFFUSION PROCESS

After establishing the hierarchical structure of all the samples by selecting representative images among local neighbor images, we only spread similarity between representative images and query images by applying diffusion process method. To accomplish the similarity diffusion of top-layer images and queries, we need to construct K nearest neighbor graph, and calculate corresponding affinity matrix of top-layer images and queries. However, computation will be double and time-consuming if we directly compute that affinity matrix by using Gaussian kernel function. Considering this, we just utilize affinity matrix of top-layer images obtained by similarity transformation matrix, as described in above Sec III.A. In order to accurately compute affinity matrix of all images which contain top-layer images and queries, the queries will be added to k nearest neighbor graph of top-layer images.

According to above operation, the affinity matrix between queries and top-layer representatives can be calculated as:

$$W_e(i) = \begin{cases} \exp\left[-d^2(y, x_i) / \sigma_2^2 \right], & if \ x_i \in knn(y) \\ 0, & otherwise \end{cases} \tag{6}$$

where W_e denotes a vector of N-dimension. N is the number of top-layer images and σ_2 is the parameter of Gaussian kernel function. Considering the fact that we have added the queries to the K nearest neighbor graph of top-layer images to obtain another nearest neighbor graph, then its corresponding affinity matrix $\tilde{W}^{[s]}$ can be computed as:

$$\tilde{W}^{[s]} = \begin{bmatrix} W_K^{[s]} & W_e \\ W_e^T & 1 \end{bmatrix} \tag{7}$$

where $W_K^{[s]}$ is the K nearest neighbor matrix of $W^{[s]}$.

It's well known that nearest neighbor graph can be used to model the local geometric structure of data. Since we can always find k nearest neighbors of each image x_i in image dataset and connect edges between x_i and its neighbors, we can measure the geometric structure of image by constructing a graph with n vertices. There are many means can be used to define the adjacency matrix $\Phi = [\phi_{ij}](i, j = 1, 2, \ldots, n)$ on this graph such as Gaussian heat kernel distance or label prior. In this paper, we choose the former, i.e., Eq.(6), to define the adjacency matrix.

Based on the above operation, the graph regularization framework for the diffusion process of all images including the query image and the top-level representative image is defined as:

$$\min_A \frac{1}{2} \sum_{i,j,k,l=1}^{N+1} \tilde{W}_{ij}^{[s]} \tilde{W}_{kl}^{[s]} \left(\frac{A_{ki}^{[s]}}{\sqrt{D_{ii}^{[s]} D_{kk}^{[s]}}} - \frac{A_{lj}^{[s]}}{\sqrt{D_{jj}^{[s]} D_{ll}^{[s]}}} \right)^2 + \mu \sum_{k,i=1}^{N} W_e(i) \cdot \left(A_{ki}^{[s]} - Y_{ki} \right)^2 \tag{8}$$

where $\mu > 0$ is a regularization parameter, A is the diffused similarity measure and D is the diagonal matrix with element $D_{ii}^{[s]} = \sum_{j=1}^{N+1} \tilde{W}_{ij}^{[s]}$. $Y \in R^{(N+1) \times (N+1)}$ denotes initial affinity values. By setting partial derivative of Eq.(8), we can obtain:

$$\left(A^{[s]} \right)^* = (1 - \alpha) \, vec^{-1} \left((I - \alpha S)^{-1} vec(Y) \right) \tag{9}$$

where S which is defined as $S = s \otimes s$ is the Kronecker product of $S = D^{-1/2} \tilde{W}^{[s]} D^{-1/2}$ with itself. $vec(\cdot)$ is an operator that vectoring a matrix by stacking the columns one after the next into a column vector and $vec(\cdot)^{-1}$ is the inverse operator of $vec(\cdot)$. α is defined as $\alpha = 1/(\mu + 1)$. The Eq.(9) can be represented as:

$$\left(A^{[s]} \right)^{(t+1)} = \alpha S \left(A^{[s]} \right)^{(t)} S^T + (1 - \alpha) \, Y \tag{10}$$

It can be observed that Eq.(10) converges to a stationary value and the initial value $\left(A^{[s]} \right)^{(1)}$ is irrelevant in diffusion iteration. By using the above iterative computation to diffuse

similarity among images, we can obtain diffused similarity matrix $A^{[s]}$ of these images. The $(N+1)$-th row of the diffused similarity matrix, that is $A^{[s]}_{N+1}$, denotes similarity between the queries and image set which contains queries and top-layer images. And the first N values of the similarity measure $A^{[s]}_{N+1}$ denotes the similarity between queries and top-layer images, we use $F^{[s]}$ denote it.

C. RELEVANCE FEEDBACK

In most of the existing diffusion process for image retrieval methods, the similarity values between pairwise images are only measured by utilizing the low-level features of images, which may not reflect the images semantics accurately. In order to overcome the mentioned semantic gap, we use relevance feedback to provide semantic information from users.

According to the first T-top retrieved images returned by ranking diffused similarity defined as $F^{[s]}$ between queries and top-layer images, users can mark returned results as positive or negative samples. If the returned image is relevant with the query image, we set the affinity value between the two images to 1; if the returned image is not relevant with the query image, we set the affinity value between the two images to -1; otherwise, the affinity value similar is set to 0. The affinity values Y_e between queries and top-layer images can be denoted as:

$$Y_e(i) = \begin{cases} 1, & if \;\; x_i \in P_T(y), \;\; i = 1, 2, \cdots, T \\ -1, & if \;\; x_i \notin N_T(y), \;\; i = 1, 2, \cdots, T \\ 0, & otherwise \end{cases} \tag{11}$$

where $P_T(y)$ and $N_T(y)$ denote the positive and negative image set, respectively. All the images in $P_T(y)$ are relevant with query image y, and all the image in $N_T(y)$ are not relevant with the query image y.

Utilizing the above positive image set P_T and negative image set N_T, we can obtain the affinity values among the top-layer images further. We define two set: $S_t = \{(x_i, x_j) | (x_i, x_j) \in P_T\}$ and $D_t = \{(x_i, x_j) \mid (x_i \in P_t \wedge x_j \in N_t) \vee (x_i \in N_t \wedge x_j \in P_T)\}$ with $\{i, j\} \in \{1, 2, \cdots, N\}$. N represents the number of top-layer images as mentioned before. Assuming that the image x_j is the query image, the image x_i and x_k are belong to the top layer, if $(x_i, x_j) \in S$, we obtain $(x_i, x_j) \in S$, that is the affinity value between these pairwise images to 1; if $(x_i, x_j) \in S$ and $(x_j, x_d) \in D$, we obtain $(x_i, x_d) \in D$, that is the affinity value between the pairwise images to -1. According to this strategy, the affinity matrix between the queries and top-layer images can be updated.

In the regularization framework Eq.(8), the matrix Y denotes the initial affinity values of all images including the queries and top-layer images. Without introducing relevance feedback, the matrix Y can be defined with identity matrix I or the original affinity matrix. After adding users' feedback, the initial affinity values of these images will change. The marked information provided by users should be used to update the matrix Y. The initial affinity values Y can be updated as follow:

$$Y = \begin{bmatrix} Y_n & Y'_e \\ Y_e & 1 \end{bmatrix} \tag{12}$$

Finally, the feedback information Y is used at the next diffusion process of the query image and the top-layer images for better retrieval performance by Eq.(10).

D. SIMILARITY TRANSFORMATION AMONG HIERARCHICAL STRUCTURE

After obtaining the diffused similarity between queries and top-layer images, the next step is to interpolate the similarity from top to bottom through interpolation matrix. The interpolation matrix between two adjacent layers is utilized as the similarity transformation matrix. The similarity between the queries and those images in the s-th layer interpolating to the $(s-1)$-th layer is defined as:

$$F^{[s-1]} = F^{[s]} Q^{[s-1]T} \tag{13}$$

where $F^{[s]}$ is the similarity measurement between query image and the images in the s-th layer, and $F^{[s-1]}$ is the similarity measurement between query image and the images in the $(s-1)$-th layer. In the same manner, the similarity measure of the rest layers can be obtained until interpolating to the bottom layer. And the final similarity measure $F^{[s]}$ between the query image and all images in database can be computed by:

$$F^{[0]} = F^{[s]} \left(Q^{[s-1]}\right)^T \left(Q^{[s-2]}\right)^T \cdots \left(Q^{[1]}\right)^T \left(Q^{[0]}\right)^T \tag{14}$$

E. SUMMARY OF THE PROPOSED ALGORITHM

In summary, to solve the semantic gap problem and improve the retrieval computational efficiency of the regularization diffusion process, we propose the graph regularized hierarchical diffusion process with relevance feedback and apply it to retrieve medical image. By constructing a bottom-to-top hierarchical structure to measure manifold structure of images, only query images and top-layer images are used to diffuse similarity among images by using regularized diffusion process. Next, the feedback information provided by users is used to improve the retrieval performance. And the similarity between query images and all images in image dataset is obtained via interpolation matrix from top to bottom. The steps of the proposed method are described in **Algorithm 1**.

IV. COMPLEXITY ANALYSIS OF THE PROPOSED ALGORITHM

In this part, we mainly compare time complexity of proposed GRHDP algorithm with existing RDP and RED algorithm. The proposed GRHDP can be decomposed into three steps, including construction of hierarchical structure, diffusion process and relevance feedback, and similarity transformation among hierarchical structure layer. Considering the fact that hierarchical structure of images in the library image

Algorithm 1 GRHDP Algorithm

Require:

Image dataset $X = \{x_1, x_2, \cdots, x_n\} \in R^{m\times n}$; query image $y \in R^{m\times 1}$.

Ensure:

The similarity $F^{[0]}$ between queries and images in X.

1: Extract features of all images;
2: Construct the k nearest neighbor graph $G^{[1]}(V^{[1]}, W^{[1]})$ of the images in image library;
3: Establish hierarchical structure of all images;
4: **for** $s = 1 : M$ **do**
5: Select representative images $V^{[s]}$ of s-th layer using Eq.(2);
6: Deliver the selected representatives $V^{[s]}$ to next layer and treat $V^{[s]}$ as candidate images;
7: Calculate interpolation matrix $Q^{[s-1]}$ from $(s-1)$-th layer to s-th layer using Eq.(3);
8: Update the representative images $V^{[s]}$ corresponding similarity matrix $W^{[s]}$ using Eq.(4);
9: **end for**
10: Calculate affinity matrix $\tilde{W}^{[s]}$ of images including query images and top-layer images using Eq.(7);
11: Diffuse similarity between queries and top-layer images using Eq.(10);
12: Mark positive or negative images of returned T top retrieved images using Eq.(11)
13: Update the initial matrix Y by Eq.(12)
14: Repeat step 11;
15: Obtain similarity $F^{[0]}$ between queries and all images in dataset using interpolation matrix;
16: **for** $s = M : 1$ **do**
17: $F^{[s-1]} = F^{[s]}\left(Q^{[s]}\right)^T$
18: **end for**

can be established offline, the time complexity of the first step does not need to be calculated. That is to say the time complexity of our method mainly focus on the analysis of the second and third step.

As analyzed in previous works, the time complexity of diffusion process and relevance feedback is $O\left(\omega N^{[M]} m t_A\right)$, where ω is the number of feedback and m denotes feature dimension. t_A and $N^{[M]}$ denote the number of iterations and top-layer images, respectively. M is the number of layer. Then, it can be calculated that the time complexity of similarity transformation among layers in hierarchical structure is $O\left(N^{[M]}N^{[M-1]} + N^{[M-1]}N^{[M-2]} + \cdots + N^{[2]}N^{[1]}\right)$. Therefore, time complexity of GRHDP can be computed as $O\left(\omega N^{[M]} m t + N^{[M]}N^{[M-1]} + \cdots + N^{[2]}N^{[1]}\right)$. Since the hierarchical structure of images is bottom-to-top structure, the number of images in each layer satisfies $N^{[M]} < N^{[M-1]} < \cdots < N^{[1]}$. Thus, we can conclude time complexity of GRHDP as:

$$O\left(\omega N^{[M]} m t_A + N^{[M]}N^{[M-1]} + \cdots + N^{[2]}N^{[1]}\right)$$
$$\ll O\left(N^{[M]} m t_A\right) + (M-1)\, O\left(\left(N^{[1]}\right)^2\right)$$
$$< O\left(\left(N^{[1]}\right)^2 m t_B\right) \quad (15)$$

It has been proved that the time complexity of RDP [21] is $O\left(\left(N^{[1]}\right)^2 m t_B\right)$, where t_B is total iteration. Reference [22] has pointed that RED is dominated by $O\left(\left(N^{[1]}\right)^3 t_B\right)$. Since $m \ll N$, then we can see that GRHDP can effectively reduce time complexity comparing with RDP and RED.

V. EXPERIMENT AND ANALYSIS

In this section, we use two medical image datasets, i.e., Brain [33] and IRMA [34], to demonstrate the validity of proposed GRHDP algorithm in medical image retrieval task. We firstly compare and analyse our method with existing representative methods, including manifold ranking (MR) [8], regularized diffusion process (RDP) [21] and regularized ensemble diffusion (RED) [22]. Then, we use the Bullseye Score (BS) to evaluate retrieval performance of these four comparisons in Brain dataset, and adopt precision and recall to evaluate the performance in IRMA dataset.

A. DATASET AND IMPLEMENTATION DETAILS

In this paper, we mainly conduct experiments on Brain and IRMA image dataset. All the experiments will be conducted on Intel(R) Core(TM) i9-9900K CPU@3.6GHz with 16 cores and NVIDIA GeForce RTX 2080Ti GPU using the same setting to ensure impartiality and objectivity.

Brain.[1] Brain is an open dataset which comprised of the atlas of the whole brain. Each scan has multiple slices with the range voxel size 3 mm to 5 mm. We downloaded 12,028 CT images to construct dataset to evaluate the retrieval performance following the previous work [33]. Considering that all the CT images are collected from 33 patients, we directly divided them into 33 categories. In the experiments, we split the Brain dataset into training, testing (image library) and query part following [33].

IRMA.[2] IRMA (Image Retrieval in Medical Applications, IRMA) is an open dataset which contains 12,677 unlabeled CT images with 193 categories and 10,000 labeled CT images with 57 categories. Select images from the labeled CT images with 57 categories for retrieval experiments. The number of different categories of images is quite different, among which there are more than 100 images in 17 categories [27]. This paper selects images from these 17 categories for experiments, and selects all images for categories with fewer than 200 images. For more than 200 images, 200 images were randomly selected from each category. A total of 3,109 images were selected. Then, divide the training set and test set according to 4:1.

According to [29], when hierarchical structure is constructed by selecting representative images for image library,

[1] http://www.med.harvard.edu/AANLIB/.
[2] http://goo.gl/NX44yh.

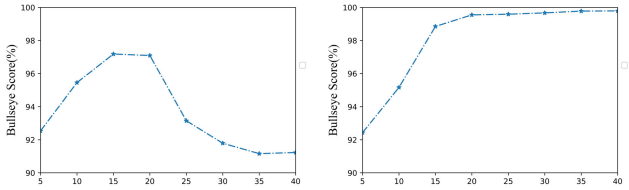

(a) BS variation with different K (b) BS variation with different k

FIGURE 2. The BS variation with different K and k values for image retrieval using GRHDP.

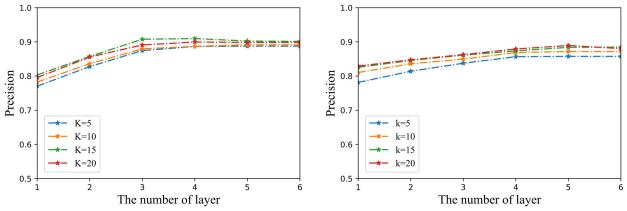

(a) Precision comparisons with k and M (b) Precision comparisons with K and M

FIGURE 3. Precision comparisons with different k, K and M using GRHDP on brain datset.

the parameters σ_1^2 and σ_2^2 are both set to be 0.1, the parameter α is set to 0.4, and the strength threshold θ is set to 0.99. The layers of hierarchical structure will be set automatically according to the validation results in the range of [1, 6] by making trade-off between accuracy and efficiency.

In order to balance the retrieval accuracy and retrieved results, radius of k nearest neighbor and K value of nearest neighbor graph will be also set automatically according to validated results. k denotes threshold radius which indicates similarity of images, i.e., if the distance of pairwise images is less than the threshold, the pairwise images are regraded as similar, otherwise they are judged to be dissimilar. K represents vertex of nearest neighbor graph, i.e., the number of images. In the experiment, the distance between the paired images was calculated using proposed convexity measurement [35] to calculate the distance.

B. EXPERIMENTAL RESULTS ON BRAIN DATASET

We firstly conduct experiments on Brain dataset and analyze the influence of different neighbor parameter k and K values on the retrieval performance of proposed GRHDP. The comparisons are shown in Figure 2, from which it can be observed that there is not clear and direct relationship between k and K from the results.

From Figure 2(a), it can be seen that a higher K may not cause a higher Bullseye score since the number of representative images in a dataset can be estimated [32]. Selecting many representatives embeds some irrelevant images into the top layer, which causes unsatisfactory retrieved images.

From Figure 2(b), we can conclude the larger is the k value, the higher is the Bullseye score. k indicates the similarity among images, Bullseye score will become more higher when adopting relatively high threshold radius. But it does not mean that the higher is k value, the better are retrieved results as well as Bullseye score. In order to balance the retrieved results and retrieval accuracy, in subsequent experiments the k and K are set to be 20 and 15, respectively.

M is the number of layer, which may be different for different datasets. As mentioned before, we set it according to the validation results in the range of [1, 6] to balance the accuracy and efficiency. The results are shown in Figure 3.

It can be observed that the larger is the M, the higher is the precision. But the increment caused by $M > 4$ is small, and constructing many layer (i.e., $M = 5$ and $M = 6$) incurs more time. Thus, we believe that $M = 4$ is the best choice for Brain dataset according to Figure 3. Then, in order to verify the contribution of relevant feedback, we also conduct experiment on Bullseye score with and without relevance feedback (RF). The results are shown in Table 1. Table 1 generally shows that when introducing relevance feedback all the comparisons can achieve better results, which verifies relevance feedback indeed promotes retrieval performance. Then, it can be observed that the Bullseye score of the proposed method is higher than that of other methods.

TABLE 1. Retrieval performance comparisons with relevance feedback (RF).

Method	BS with RF(%)	BS without RF(%)
MR [8]	84.13	78.67
RDP [21]	86.33	81.45
RED [22]	87.99	83.68
GRHDP(ours)	89.10	86.31

TABLE 2. Retrieval performance comparisons with different feedback times.

Method	$N = 1$	$N = 2$	$N = 3$	$N = 4$	$N = 5$
MR [8]	84.13	87.92	89.75	89.76	88.96
RDP [21]	86.33	88.45	90.13	90.67	90.86
RED [22]	87.99	89.68	92.13	92.67	93.19
GRHDP(ours)	89.10	93.33	95.47	95.65	96.04

It's not hard to imagine that the more is the manual participation, the better is the retrieval performance. But the more manual participation indicates worse flexibility. In order to make the trade off between feedback times and precision, we have also investigated some GRHDP variants by introducing relevance feedback to discuss the relationship between feedback times and precision. The results are shown in Table 2, where N denotes the number of feedback times. According to prior, if $N > 5$, the users become impatient. So, we fix N in the range of [0, 5].

Table 2 indicates that the more is the feedback time, the higher is the precision, which is general knowledge in image retrieval. As mentioned above, considering the acceptable human participation and satisfactory precision, we investigate and compare the increments of using different feedback times. The results are shown in Table 3.

It is no hard to find that more feedback times can indeed bring higher precision. But the increment is tiny when the

TABLE 3. Increment comparisons using different feedback times.

Method	0←1	1←2	2←3	3←4	4←5
MR [8]	6.94%	4.59%	2.09%	0	0.02%
RDP [21]	5.99%	2.45%	1.89%	0.06%	0.02%
RED [22]	5.15%	1.92%	2.73%	0.05%	0.05%
GRHDP(ours)	6.23%	4.74%	2.29%	0.01%	0.04%

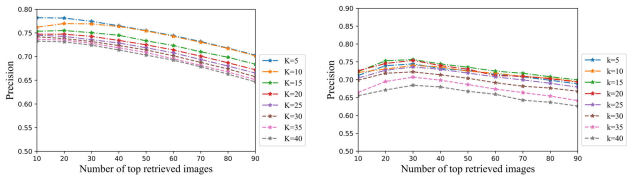

(a) Precision comparisons with K and different top retrieved images (b) Precision comparisons with k and different top retrieved images

FIGURE 4. Precision comparisons with different *K*, *k* and the number of top retrieved images using GRHDP on IRMA datset.

feedback time exceeds 3. Combining all the results in this Section, we can conclude the following two conclusions:

(1) Comparing with the methods without feedback, the retrieval performance of the methods with feedback has been significantly improved;

(2) There is no need to conduct too many relevance feedback times, which will cause small precision increment and worse flexibility.

C. EXPERIMENTAL RESULTS ON IRMA DATASET

After inheriting above two conclusions, we compare GRHDP with other comparisons on IRMA dataset in retrieved precision and recall evaluation this part. Considering the fact that different datasets have different manifold structures, which requires different threshold radiuses (i.e., K). We use different threshold radius K values for medical image retrieval on IRMA dataset using our GRHDP to study the influence of different K. The comparisons are shown in Figure 4.

From Figure 4(a), we can see that precision of GRHDP is the highest when the number of returned images is less than 50 with $K = 5$. When the number of retrieved images is greater than or equal to 50, the precisions of GRHDP with $K = 5$ and $K = 10$ are approximately equal, and both greater than that of GRHDP with other K values.

From Figure 4(b), we can see that the precisions of GRHDP with $K < 25$ are approximately equal. Considering the constructing time of near neighbor matrix and precision increment, we set $k = 15$. According to the results in Figure 3, in subsequent experiments the threshold radius K and k value are fixed to be 5 and 15, respectively.

Since we have discussed the setting of threshold radius k and K value of nearest neighbor, now we conduct some experiments to discuss the number of layer in IRMA dataset. We follow the same setting in original papers. The results are shown in Figure 5.

From Figure 5, we can see that $M = 5$ is suitable for IRMA dataset, which is different from Brain dataset. After

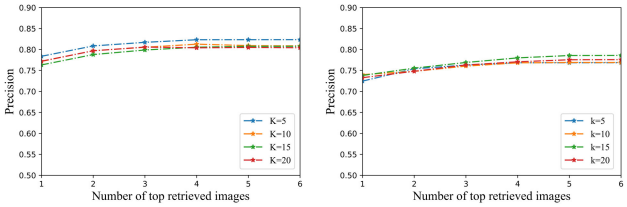

(a) Precision comparisons with K and M (b) Precision comparisons with k and M

FIGURE 5. Precision comparisons with different *K*, *k* and *M* using GRHDP on IRMA datset.

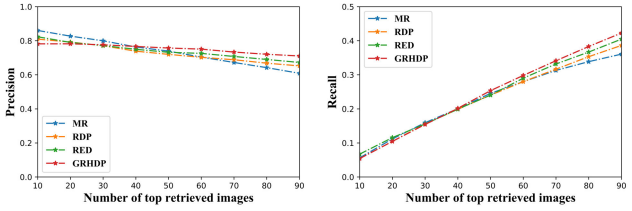

(a) Precision Curve (b) Recall Curve

FIGURE 6. Comparisons of precision and recall for image retrieval on IRMA dataset without feedback.

determining the K value and the number of layer, we compare the retrieval performance of all comparisons on IRMA dataset. Figure 6-8 show the retrieval performance results of all the comparisons on IRMA dataset. From these results we can obtain three conclusions:

(1) With increment of returned images, the difference of precision between GRHDP and three comparison methods becomes bigger. A similar trend can be found in recall;

(2) The precision obtained by our method drops slower than that of other comparisons;

(3) The greater the amount is the feedback, the higher are precision and recall.

If using standard regularization adopted in RDP [21] and RED [22], it concentrates both related and undetermined images into nearest neighbor graph. There are less related images locate in the nearest neighbor when the number of returned image increasing, which means that nearest neighbor matrix constructed by corresponding graph become sparse. In contrast, our method embeds graph regularization into similarity preservation, which only concentrates the related images into nearest neighbor graph. The related images in nearest neighbor matrix constructed by ours is less sparser than that of other comparisons. Thus, it results in dramatic drops comparing with our method. It can be also explained the first conclusion, which mainly owns to graph regularization.

As shown in Figure 6, when without introducing relevance feedback and the number of returned image is more than 40, precision and recall of GRHDP are higher than these of other comparisons. As shown in Figure 7-8, when introducing one and two feedbacks, the number decrease to be 30 and 20, respectively.

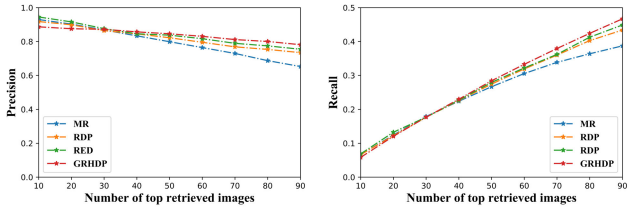

(a) Precision Curve (b) Recall Curve

FIGURE 7. Comparisons of precision and recall for image retrieval on IRMA dataset with one feedback.

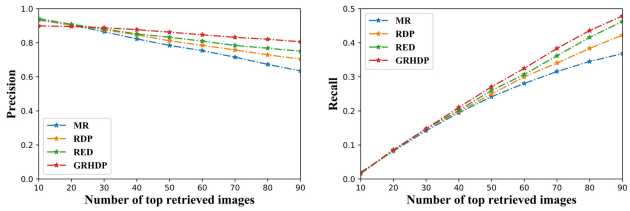

(a) Precision Curve (b) Recall Curve

FIGURE 8. Comparisons of precision and recall for image retrieval on IRMA dataset with two feedback.

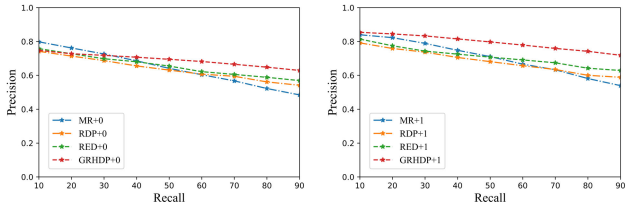

(a) Retrieval Results Comparisons without feedback (b) Retrieval Results Comparisons with one feedback

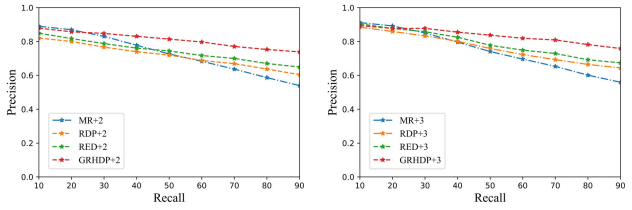

(c) Retrieval Results Comparisons with two feedback (d) Retrieval Results Comparisons with three feedback

FIGURE 9. The P-R results of comparison methods with different feedback times in medical image retrieval.

Apart from these three conclusions, we can also see that the initial precision or recall with less 20 returned images are comparable, which indicates that our method does not have clear advantages comparing with other methods at the initial stage since it does not use any prior or clustering method to determine representations. However, ours achieves less time complexity than RDP or RED as analyzed before. Owning to the introduction of graph regularization and relevance feedback, ours obtain better retrieval performance with the increasing of the number of returned images.

As mentioned before, the more is the feedback times, the better is the retrieval performance. In order to balance the manual participation and precision, we have also conducted some experiments to reveal it. The results are shown in Figure 9.

When $N > 3$, the difference caused by feedback is relatively small. That is to say, $N = 3$ is regarded as best feedback times under the acceptable feedback times and good precision, which is consistent with the previous conclusions.

From all above results, we can obtain that the precision-recall results of our GRHDP is more higher and stabler than these of other comparisons when setting same feedback time and top retrieved images. Besides, the retrieval performance can be further improved with the introduction of relevance feedback which should be set as small as possible for the balance between retrieval performance and fussy human participation.

D. LIMITATION AND DISCUSSION

Although our proposed GRHDP shows the superiority in retrieving medical images comparing with other hierarchical diffusion process-based methods, some limitations should be taken into consideration in our next work. Firstly, we only use the basic framework and traditional feature to represent images, which could be further improved, for example, by using state-of-the-art stack auto-encoder [27] or recently proposed parallel convolutional neural network [28]. Then, the initial performance is not satisfactory since the proposed method adopts randomly adaptive way to determine the representative images. We believe that its complementarity and users feedback to other methods (such as density peak clustering) can be further exploited to improve capacity for medical image retrieval. Thirdly, it currently has not been evaluated on multi-modal multi-dimension medical images (e.g., 3D MRI, CT and PET). In order to achieve this, combining the nearest neighbor graph and the similarity between inter- and intra-modal image could be helpful for retrieval performance. All these three discussion will be researched in our future studies.

VI. CONCLUSION

In this paper, we propose a novel graph regularized hierarchical diffusion process with relevance feedback for medical image retrieval method, which mainly addressed the problems of expensive computation for large-scale image retrieval and semantic gap by utilizing algebraic multi-grid and relevance feedback. All the images are model as hierarchical structure by selecting representative images where top-layer images are involved in diffusion process with the query image. Then semantic information provided by users is used to diffuse similarity among images again. Finally, the diffused similarity measure is interpolated from top-to-bottom to obtain the similarity values between the query image and all images of the image library. The extensive experiments on Brain and IRMA dataset show that our proposed GRHDP gains better retrieval performance

comparing with other recent state-of-the-art diffusion process-based algorithms.

ACKNOWLEDGMENT

The authors would like to thank the anonymous reviewers for their help.

REFERENCES

[1] A. Purbey, M. Sharma, and B. Bohra, "Review on: Content-based image retrieval," *Int. J. Sci., Eng. Res.*, vol. 8, no. 1, pp. 510–514, 2017.

[2] R. Ashraf, M. Ahmed, S. Jabbar, S. Khalid, A. Ahmad, S. Din, and G. Jeon, "Content based image retrieval by using color descriptor and discrete wavelet transform," *J. Med. Syst.*, vol. 42, no. 3, pp. 44–56, Mar. 2018.

[3] S. T. Roweis, "Nonlinear dimensionality reduction by locally linear embedding," *Science*, vol. 290, no. 5500, pp. 2323–2326, Dec. 2000.

[4] M. S. Mirasadi and A. H. Foruzan, "Content-based medical image retrieval of CT images of liver lesions using manifold learning," *Int. J. Multimedia Inf. Retr.*, vol. 8, no. 4, pp. 233–240, Dec. 2019.

[5] D. C. G. Pedronette, Y. Weng, A. Baldassin, and C. Hou, "Semi-supervised and active learning through manifold reciprocal kNN graph for image retrieval," *Neurocomputing*, vol. 340, pp. 19–31, May 2019.

[6] R. Liu, Y. Zhao, and S. Wei, "Enhance neighbor reversibility in subspace learning for image retrieval," *IEEE J. Sel. Topics Signal Process.*, vol. 12, no. 6, pp. 1338–1350, Dec. 2018.

[7] H. Shen, D. Tao, and D. Ma, "Multiview locally linear embedding for effective medical image retrieval," *PLoS ONE*, vol. 8, no. 12, Dec. 2013, Art. no. e82409.

[8] Q. H. Van, H. T. Van, H. N. Hoang, T. D. Van, and S. Ablameyko, "A modified efficient manifold ranking algorithm for large database image retrieval," *Nonlinear Phenomena Complex Syst.*, vol. 23, no. 1, pp. 79–89, Apr. 2020.

[9] P. Soundalgekar, M. Kulkarni, D. Nagaraju, and S. Kamath, "Medical image retrieval using manifold ranking with relevance feedback," in *Proc. IEEE 12th Int. Conf. Semantic Comput. (ICSC)*, Jan. 2018, pp. 369–375.

[10] J. Wu, Y. He, X. Guo, Y. Zhang, and N. Zhao, "Heterogeneous manifold ranking for image retrieval," *IEEE Access*, vol. 5, pp. 16871–16884, 2017.

[11] B. Xu, J. Bu, C. Chen, C. Wang, D. Cai, and X. He, "EMR: A scalable graph-based ranking model for content-based image retrieval," *IEEE Trans. Knowl. Data Eng.*, vol. 27, no. 1, pp. 102–114, Jan. 2015.

[12] J. Wu, Y. Li, Y. Sang, and H. Shen, "Incorporating manifold ranking with active learning in relevance feedback for image retrieval," in *Proc. 13th Int. Conf. Parallel Distrib. Comput., Appl. Technol.*, Dec. 2012, pp. 739–744.

[13] D. Lin, V. J. Wei, and R. C.-W. Wong, "First index-free manifold ranking-based image retrieval with output bound," in *Proc. IEEE Int. Conf. Data Mining (ICDM)*, Nov. 2019, pp. 1216–1222.

[14] X. Bai, X. Yang, L. J. Latecki, W. Liu, and Z. Tu, "Learning context-sensitive shape similarity by graph transduction," *IEEE Trans. Pattern Anal. Mach. Intell.*, vol. 32, no. 5, pp. 861–874, May 2010.

[15] J. Jiang, B. Wang, and Z. Tu, "Unsupervised metric learning by self-smoothing operator," in *Proc. Int. Conf. Comput. Vis.*, Nov. 2011, pp. 794–801.

[16] Y. Li, X. Kong, H. Fu, and Q. Tian, "Node-sensitive graph fusion via topo-correlation for image retrieval," *IEEE Trans. Circuits Syst. Video Technol.*, vol. 30, no. 10, pp. 3777–3787, Oct. 2020.

[17] S. Bai, X. Bai, Q. Tian, and L. J. Latecki, "Regularized diffusion process on bidirectional context for object retrieval," *IEEE Trans. Pattern Anal. Mach. Intell.*, vol. 41, no. 5, pp. 1213–1226, May 2019.

[18] J. Wang, Y. Li, X. Bai, Y. Zhang, C. Wang, and N. Tang, "Learning context-sensitive similarity by shortest path propagation," *Pattern Recognit.*, vol. 44, nos. 10–11, pp. 2367–2374, Oct. 2011.

[19] X. Yang, L. Prasad, and L. J. Latecki, "Affinity learning with diffusion on tensor product graph," *IEEE Trans. Pattern Anal. Mach. Intell.*, vol. 35, no. 1, pp. 28–38, Jan. 2013.

[20] M. Donoser and H. Bischof, "Diffusion processes for retrieval revisited," in *Proc. IEEE Conf. Comput. Vis. Pattern Recognit.*, Jun. 2013, pp. 1320–1327.

[21] S. Bai, X. Bai, Q. Tian, and L. J. Latecki, "Regularized diffusion process for visual retrieval," in *Proc. AAAI Conf. Artif. Intell.*, 2017, pp. 3967–3973.

[22] S. Bai, Z. Zhou, J. Wang, X. Bai, L. J. Latecki, and Q. Tian, "Automatic ensemble diffusion for 3D shape and image retrieval," *IEEE Trans. Image Process.*, vol. 28, no. 1, pp. 88–101, Jan. 2019.

[23] F. Yang, B. Matei, and L. S. Davis, "Re-ranking by multi-feature fusion with diffusion for image retrieval," in *Proc. IEEE Winter Conf. Appl. Comput. Vis.*, Jan. 2015, pp. 572–579.

[24] Y. Tang, H. Wang, K. Guo, Y. Xiao, and T. Chi, "Relevant feedback based accurate and intelligent retrieval on capturing user intention for personalized Websites," *IEEE Access*, vol. 6, pp. 24239–24248, 2018.

[25] J. Wang, T. Zhang, j. song, N. Sebe, and H. Tao Shen, "A survey on learning to hash," *IEEE Trans. Pattern Anal. Mach. Intell.*, vol. 40, no. 4, pp. 769–790, Apr. 2018.

[26] O. Pelka, F. Nensa, and C. M. Friedrich, "Annotation of enhanced radiographs for medical image retrieval with deep convolutional neural networks," *PLoS ONE*, vol. 13, no. 11, Nov. 2018, Art. no. e0206229.

[27] S. Öztürk, "Stacked auto-encoder based tagging with deep features for content-based medical image retrieval," *Expert Syst. Appl.*, vol. 161, Dec. 2020, Art. no. 113693.

[28] A. Qayyum, S. M. Anwar, M. Awais, and M. Majid, "Medical image retrieval using deep convolutional neural network," *Neurocomputing*, vol. 266, no. 29, pp. 8–20, Nov, 2017.

[29] X. Zeng, M. Hu, and S. Zhu, "Image retrieval based on hierarchical locally constrained diffusion process," in *Proc. IEEE Int. Conf. Big Knowl. (ICBK)*, Aug. 2017, pp. 290–296.

[30] M. Kokare, P. K. Biswas, and B. N. Chatterji, "Texture image retrieval using new rotated complex wavelet filters," *IEEE Trans. Syst., Man Cybern. B, Cybern.*, vol. 35, no. 6, pp. 1168–1178, Dec. 2005.

[31] X. Gao, X. Shi, G. Zhang, J. Lin, M. Liao, K.-C. Li, and C. Li, "Progressive image retrieval with quality guarantee under MapReduce framework," *IEEE Access*, vol. 6, pp. 44685–44697, 2018.

[32] E. Sharon, M. Galun, D. Sharon, R. Basri, and A. Brandt, "Hierarchy and adaptivity in segmenting visual scenes," *Nature*, vol. 442, no. 7104, pp. 810–813, Aug. 2006.

[33] L. Xu, X. Zeng, H. Zhang, W. Li, J. Lei, and Z. Huang, "BPGAN: Bidirectional CT-to-MRI prediction using multi-generative multi-adversarial nets with spectral normalization and localization," *Neural Netw.*, vol. 128, pp. 82–96, Aug. 2020.

[34] J. Han and L. Guo, "A new image retrieval system supporting query by semantics and example," in *Proc. Int. Conf. Image Process.*, Sep. 2002, pp. 953–956.

[35] R. R. Gopalan, P. P. Turaga, and R. R. Chellappa, "Articulation-invariant representation of non-planar shapes," in *Proc. Eur. Conf. Comput. Vis.*, Heraklion, Crete, 2010, pp. 286–299.

LIMING XU received the B.S. and M.S. degrees in computer science and technology from China West Normal University, China, in 2014 and 2017, respectively. He is currently pursuing the Ph.D. degree with the Department of Computer Science and Technology, Chongqing University of Posts and Telecommunications. His research interests include machine learning, adversarial learning, image processing, and learning to hash.

XIAOPENG YAO graduated from the School of Manufacturing Science and Engineering, Sichuan University, Chengdu, in June 2014. He received the Ph.D. degree in mechatronic engineering. He is currently a Vice Professor with Southwest Medical University. His research interests include image processing and medical big data analysis.

LISHA ZHONG graduated from Chongqing University, Chongqing, China, in July 2008. She received the M.S. degree from Chongqing University, in July 2011. She is currently pursuing the Ph.D. degree with the Chongqing University of Posts and Telecommunications. She is also a Teacher with Southwest Medical University. Her research interests include image and signal processing and analysis.

JIANBO LEI received the M.S. degree in computer sciences and the M.A. degree in medical informatics from Columbia University, and the Ph.D. degree in biomedical informatics from The University of Texas Health Science Center. He was a Pediatrician with the Peking Union Medical College Hospital. He is currently a Professor and the Founding Executive Director of Peking University Center for Medical Informatics. He is also one of the leading informatics scientists in health domain in China. His research interests include diverse, including hospital information systems, health big data mining, natural language processing, medical image processing, wearable devices, health management, CDSS, and so on.

ZHIWEI HUANG graduated from the Department of Mechanical Engineering, North University of China, Taiyuan, China, in July 2001. He received the M.S. degree from the School of Electronics and Mechanical Engineering and the School of Manufacturing Science and Engineering, Sichuan University, in July 2006. He is currently pursuing the Ph.D. degree with the Chongqing University of Posts and Telecommunications. He is also a Vice Professor with Southwest Medical University. His research interest includes image processing analysis by means of artificial intelligence.